Localization of the K^+ Lock-In and the Ba^{2+} Binding Sites in a Voltage-gated Calcium-modulated Channel

Implications for Survival of K^+ Permeability

Cecilia Vergara,*‡ Osvaldo Alvarez,*‡ and Ramon Latorre*‡§

From the *Departmento de Biología, Facultad de Ciencias, Universidad de Chile, Casilla 653, Santiago, Chile; ‡Centro de Estudios Científicos de Santiago, Casilla 16443, Santiago 9, Chile; and §Department of Anesthesiology, University of California Los Angeles, Los Angeles, California 90095-1778

abstract Using Ba^{2+} as a probe, we performed a detailed characterization of an external K^+ binding site located in the pore of a large conductance Ca^{2+}-activated K^+ (BK_{Ca}) channel from skeletal muscle incorporated into planar lipid bilayers. Internal Ba^{2+} blocks BK_{Ca} channels and decreasing external K^+ using a K^+ chelator, (+)-18-Crown-6-tetracarboxylic acid, dramatically reduces the duration of the Ba^{2+}-blocked events. Average Ba^{2+} dwell time changes from 10 s at 10 mM external K^+ to 100 ms in the limit of very low [K^+]. Using a model where external K^+ binds to a site hindering the exit of Ba^{2+} toward the external side (Neyton, J., and C. Miller. 1988. *J. Gen. Physiol.* 92:549–568), we calculated a dissociation constant of 2.7 μM for K^+ at this lock-in site. We also found that BK_{Ca} channels enter into a long-lasting nonconductive state when the external [K^+] is reduced below 4 μM using the crown ether. Channel activity can be recovered by adding K^+, Rb^+, Cs^+, or NH_4^+ to the external solution. These results suggest that the BK_{Ca} channel stability in solutions of very low [K^+] is due to K^+ binding to a site having a very high affinity. Occupancy of this site by K^+ avoids the channel conductance collapse and the exit of Ba^{2+} toward the external side. External tetraethylammonium also reduced the Ba^{2+} off rate and impeded the channel from entering into the long-lasting nonconductive state. This effect requires the presence of external K^+. It is explained in terms of a model in which the conduction pore contains Ba^{2+}, K^+, and tetraethylammonium simultaneously, with the K^+ binding site located internal to the tetraethylammonium site. Altogether, these results and the known potassium channel structure (Doyle, D.A., J.M. Cabral, R.A. Pfuetzner, A. Kuo, J.M. Gulbis, S.L. Cohen, B.T. Chait, and R. MacKinnon. 1998. *Science.* 280:69–77) imply that the lock-in site and the Ba^{2+} sites are the external and internal ion sites of the selectivity filter, respectively.

key words: K_{Ca} channel • multiple occupancy • barium block • tetraethylammonium • lipid bilayer

introduction

The large conductance Ca^{2+}-activated K^+ (BK_{Ca})[1] channel has a multi-ion pore (Yellen, 1984b; Eisenmann et al., 1986; Cecchi et al., 1987; Neyton and Miller, 1988a,b), like many other potassium channels (Hodgkin and Keynes, 1955; Stampe and Begenisich, 1996; Doyle et al., 1998). Neyton and Miller (1988b) reached the conclusion that the pore of BK_{Ca} channels can accommodate several K^+ ions and that the K^+ sites are of high affinity. In particular, they functionally characterized a high affinity K^+ binding site facing the external solution; this site was revealed by the observation that increasing external [K^+] slows down the rate of Ba^{2+} exit from the channel (Neyton and Miller, 1988a). It is easy to interpret this observation by assuming that there is a K^+ binding site located externally to the blocking site. When the channel is blocked by Ba^{2+}, the outer K^+ site is in equilibrium with the external [K^+] so that, at very low external [K^+], the site remains empty most of the time and Ba^{2+} can exit toward the external side more easily than to the internal side. This external K^+ site was dubbed the "lock-in" site. In this study, we have determined the dissociation constant for K^+ at the lock-in site with increased accuracy by lowering the external [K^+] below the contamination level with a crown ether that binds K^+ with high affinity. The value we obtained for the dissociation constant, 2.7 μM, indicates that K^+ binding is approximately fivefold stronger than reported by Neyton and Miller (1988a). These results suggest that BK_{Ca} channels bind K^+ as tightly as Ca^{2+} channels bind Ca^{2+} ions (Dang and McCleskey, 1998). In this study, we also found that the mean Ba^{2+} blocked time is affected by tetraethylammonium (TEA^+). The stabilizing effect of TEA^+ on Ba^{2+} block is mainly due to a "trapping" of K^+ in the lock-in site.

The large conductance Ca^{2+}-activated K^+ channel has a high degree of identity in the pore region with

Address correspondence to: Ramon Latorre, Ph.D., Centro de Estudios Científicos de Santiago, Casilla 16443, Las Condes, Santiago 9, Chile. Fax: 562-233-8336; E-mail: ramon@cecs.cl

[1]*Abbreviations used in this paper:* BK_{Ca}, large conductance Ca^{2+}-activated K^+; MOPS, 3-[*N*-morpholino]propane-sulfonic acid; NMDG, *N*-methyl d-glucamine; TEA^+, tetraethylammonium.

voltage-dependent K^+ channels. The crystal structure of a K^+ channel from bacteria was recently elucidated (Doyle et al., 1998). It revealed that the bacterial K^+ channel could contain three K^+ ions in its conduction pathway. One K^+ ion was detected in a large water-filled cavity at the center of the pore near the cytoplasmic end of the selectivity filter. The other two were located at opposite ends of the selectivity filter, stabilized by backbone carbonyl groups. The TEA^+ binding site, which is located outside the selectivity filter, is made by a ring of four tyrosines near the extracellular end of the pore. Our results imply that TEA, K^+, and Ba^{2+} ions can coexist in the BK_{Ca} channel pore and set molecular constraints on the location of the lock-in and the Ba^{2+} sites. A picture that is consistent with our results and the potassium channel crystal structure (Doyle et al., 1998) is one in which the lock-in site corresponds to the K^+ site located on the extracellular side of the selectivity filter, and Ba^{2+} binds to a site on the internal side of the selectivity filter.

Despite the similarity with voltage-dependent K^+ channels, BK_{Ca} channels do not show external K^+-dependent phenomena such as C-type inactivation (López-Barneo et al., 1993) or the loss of functional channels after removal of K^+ ions from both sides of the membrane (e.g., Almers and Armstrong, 1980). Actually, it is possible to record BK_{Ca} channel activity for periods of hours without a hint of inactivation (e.g., Candia et al., 1992). A possible explanation for the stability of channels in the virtual absence of K^+ is their avidity for K^+ ions. In other words, the affinity of the channel for K^+ is so high that the low $[K^+]$ present in nominally "K^+-free" solutions ($\approx$4 μM) is sufficient to saturate the relevant K^+ binding site(s) in the pore. To test this hypothesis, we have lowered the external $[K^+]$ below the K^+-contamination level using a crown ether that chelates K^+ with high affinity. Our results show that when channels are exposed to external solutions containing less than 4 μM, K^+ channel electrical activity suddenly ceases, a result that is consistent with our hypothesis.

methods

Lipid Bilayers and Channel Incorporation

All measurements were performed on planar bilayers with a single BK_{Ca} channel inserted. Since depolarizing voltages and cytoplasmic Ca^{2+} activates BK_{Ca} channels, the "internal" side of the membrane was defined according to the voltage and Ca^{2+} dependence of the channel. Accordingly, the physiological voltage convention is used throughout, with the external side of the channel defined as zero voltage. Bilayers were cast from an 8:2 mixture of 1-palmitoyl, 2-oleoyl phosphatidylethanolamine (POPE) and 1-palmitoyl, 2-oleoyl phosphatidylcholine (POPC) in decane. Lipids were obtained from Avanti Polar Lipids. Bilayers were formed in 0.01 M 3-[*N*-morpholino]propane-sulfonic acid-*N*-methyl d-glucamine (MOPS-NMDG), pH 7. Concentrated KCl and $CaCl_2$ were added to the internal solution to a final concentration of 0.1 M and 125 μM, respectively. The internal $[Ca^{2+}]$ used fully activates the BK_{Ca} channel from skeletal muscle (e.g., Moczydlowski and Latorre, 1983). In some experiments Ba^{2+} (75–200 nM) was added to the internal solution to increase the probability of Ba^{2+} blockade events.

Rat skeletal muscle was used to prepare membrane vesicles containing BK_{Ca} channels as previously described (Latorre et al., 1982). Membrane vesicles were added very close to the bilayer and, once a channel incorporated, concentrated MOPS-NMDG, pH 7, and EGTA-NMDG were added to the extracellular side to a final concentration of 0.11 M and 400 μM, respectively. Single channel currents were recorded at 0 mV.

Data Acquisition and Analysis

Single-channel recordings were acquired using a custom-made current-to-voltage converter amplifier (Cecchi et al., 1987) connected to the solution through agar bridges made with ultrapure NaCl (Alfa Aesar). Continuous single-channel current records (3–30 min) were filtered at 400 Hz and digitized at 500 μs/point. Open and closed events were identified using a discriminator located at 50% of the open-channel current. Dwell-time histograms were logarithmically binned and fitted to a sum of exponential probability functions with Pclamp 6 software (Axon Instrument, Inc.). Closed dwell-time histograms were fitted to the sum of two exponential functions. The slow component is a Ba^{2+} block previously described in detail (Vergara and Latorre, 1983; Miller et al., 1987; Neyton and Miller, 1988a). The mean Ba^{2+} blocked times were measured in the range of 2×10^{-8} to 10^{-2} M K^+. Data were grouped in decades of K^+ concentration and the average of the logarithms of mean blocked time and the average of the logarithm of the K^+ concentrations ± SD were used in Fig. 2. The mean Ba^{2+}-blocked data obtained at various external $[K^+]$ were described using the equation (Neyton and Miller, 1988a):

$$\tau_{0-Ba} = (1/[k_{in} + k_{ext}/(1 + [K]/K_d^K)]), \quad (1)$$

where k_{in} is the dissociation rate constant toward the internal side and k_{ext} is the dissociation rate constant toward the external side of the channel when the lock-in site is empty, and K_d^K is the dissociation constant for K^+ from the channel containing a K^+ and a Ba^{2+} simultaneously. We used a nonlinear least-square fit procedure to find the values of k_{in}, k_{ext}, and K_d^K, where the statistical weight of each point was the number of observations on each decade (Alvarez et al., 1992).

Solutions

Determination of the free K^+ concentration in solutions containing low K^+ and crown ether requires knowledge of the $[K^+]$ of "K^+-free" solutions and the dissociation constant of the K^+-crown ether in the presence of 0.11 M MOPS-NMDG. The $[K^+]$ was determined using an ion-specific electrode (Orion 9319BN; Orion Research, Inc.) that is linear in the $[K^+]$ range between 1 μM and 1 M. The average K^+ contamination of the MOPS-NMDG solutions used in the present study was 4.4 μM. The contaminating $[K^+]$ of the stock of MOPS-NMDG and EGTA-NMDG solutions was also determined by atomic absorption spectrophotometry. A crown ether (a gift from Dr. Jacques Neyton, Laboratoire de Neurobiologie, Ecole Normale Supérieure, Paris, France), (+)-18-Crown-6-tetracarboxylic acid (18C6TA) from Merck, was used to chelate the contaminating external K^+ and contaminating Ba^{2+} in the internal solution. The 18C6TA:cation stoichiometry is 1:1 (e.g., Díaz et al., 1996). The crown ether binds K^+, Ca^{2+}, and Ba^{2+} with dissociation constants of 3.3×10^{-6}, 10^{-8}, and 1.6×10^{-10} M, respectively (Dietrich, 1985; Díaz et al. 1996; Neyton,

1996). The dissociation constant of the K-crown ether complex in the presence of 0.11 M MOPS-NMDG was 6.3×10^{-6} M. This value was obtained using an ion-specific electrode to measure the free $[K^+]$ in solutions of known concentrations of total K^+ and crown ether. The dissociation constant of the Ba-crown ether complex in the presence of 150 mM KCl was considered to be 1.6×10^{-10} M (Díaz et al., 1996; Neyton 1996).

results

Lowering External $[K^+]$ Modifies Slow Ba^{2+} Block, Induces the Appearance of a Flickering Ba^{2+} Block, and Alters the Channel-gating Kinetics

Fig. 1 shows K^+ currents from single BK_{Ca} channel recordings with 70 nM internal $[Ba^{2+}]$ and different external K^+ concentrations along with the corresponding closed dwell time histograms. Three different features are evident from the figure. (a) There is a slow internal Ba^{2+} block described previously[2] (Vergara and Latorre, 1983; Miller et al., 1987; Neyton and Miller, 1988a,b). Low concentrations (~70 nM) of internal Ba^{2+} induce long-lived nonconducting intervals separated by "bursts" of channel activity (clearly seen in Fig. 1, top). At the largest external $[K^+]$ used, the open probability inside a burst is close to 1. Vergara and Latorre (1983) showed that each of these long-lived blocked events represents the binding of a single Ba^{2+} ion to the channel, and they presented strong evidence that the site of Ba^{2+} binding is located within the conduction pore. (b) There is an increase in the number of fast closing

[2]Barium is effective from either side of the membrane, but is much more potent when applied to the internal solution. At zero applied voltage, the association rate constant for internally applied Ba^{2+} is ~50× higher than that for external Ba^{2+}, while the dissociation rate does not depend on the side of application (Vergara and Latorre, 1983).

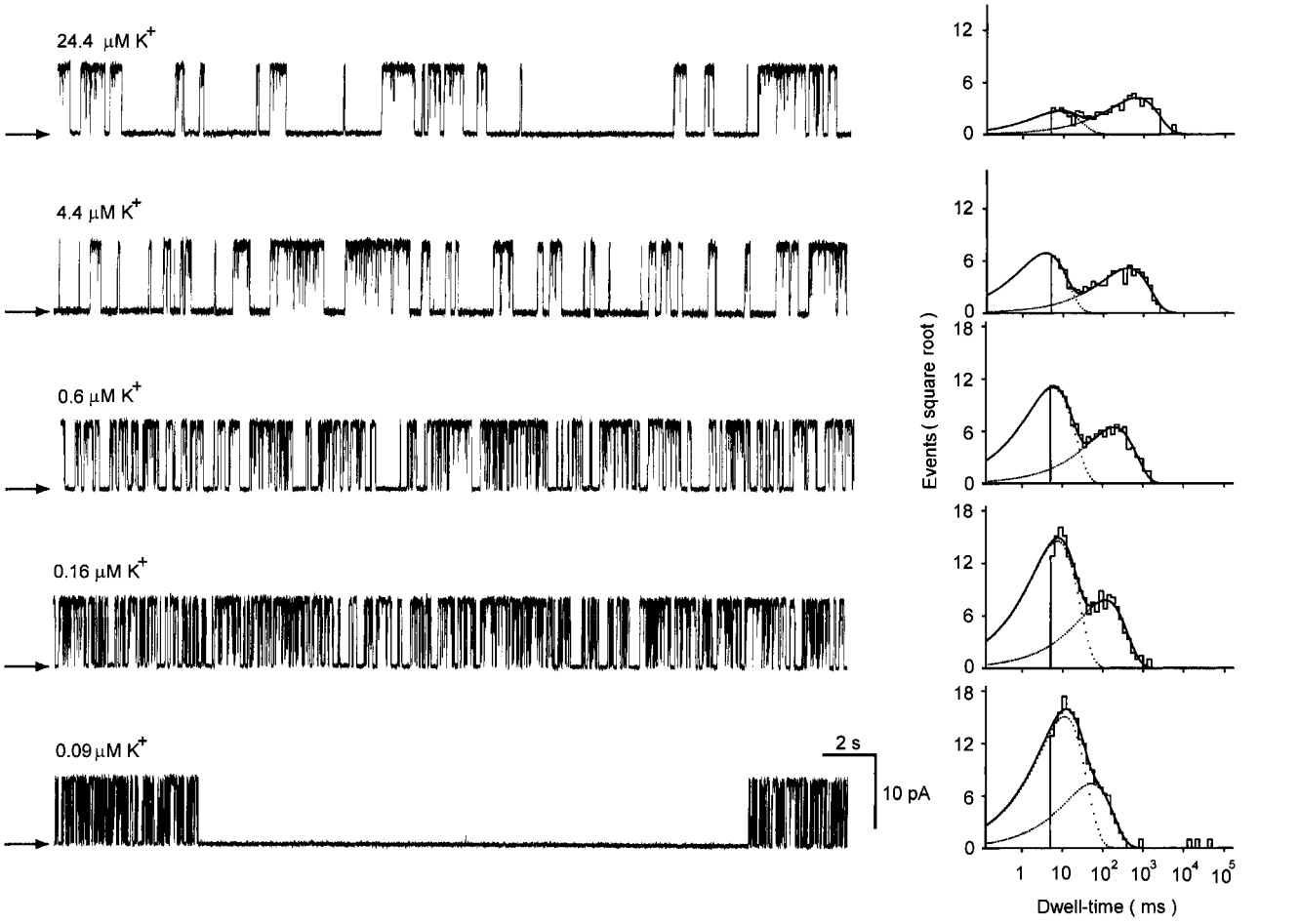

Figure 1. External K^+ affects fast and slow Ba^{2+} block and at very low $[K^+]$ a new closed state appears. (Left) 30-s single channel current traces obtained at 0 mV at different $[K^+]_{ext}$ from a single experiment. $[Ba^{2+}]_{int}$ was ~70 nM. (Right) The corresponding closed dwell time distributions of the events collected for 216 s. Dwell time distributions were truncated, leaving out all the events lasting <5 ms, and were fitted with two exponential functions. The total number of events collected, the mean dwell time (MDT) of each distribution, and the relative fraction of the two exponentials are: at 24.4 μM K^+_{ext}, 891 events with MDT of 8 (28%) and 660 (72%) ms; at 4.4 μM K^+_{ext}, 1,566 events with MDT of 4 (64%) and 411 (36%) ms; at 0.6 μM K^+_{ext}, 3,448 events with MDT of 6 (75%) and 193 (25%) ms; at 0.16 μM K^+_{ext}, 5,476 events with MDT of 7 (78%) and 113 (22%) ms; and at 0.09 μM K^+_{ext}, 6,050 events with MDT of 11 (81%) and 50 (19%) ms. At 0.09 μM K^+, four events of much longer duration were evident. The time constant for this new closed state obtained from 45-min single channel current records was 24 s.

events with decreasing external [K^+], clearly revealed by an increase in the size of the fast component of the closed dwell-time distributions (Fig. 1, right). This increase in the number of fast closing events has not been described before and, as discussed below, may be due to a change in channel kinetics or to a fast Ba^{2+} blockade. (c) A long-lasting closed state appears at very low external [K^+] (Fig. 1, bottom, and see also Fig. 3).

Slow Ba^{2+} block. Fig. 1, right, shows that the distribution of dwell times in the closed state is multiexponential. Note that mean block times of the slow component became shorter and the number of events increased as the external [K^+] was decreased. Upon decreasing the external [K^+] from 24 to 0.09 μM, the mean Ba^{2+} blocked time decreased from 660 to 50 ms. Fig. 2 shows a fit to the $\tau_{o\text{-}Ba}$-$[K^+]_{ext}$ data using Eq. 1. The best fit was obtained with $k_{ext} = 7.6 \pm 1.7\ s^{-1}$, $k_{in} = 0.11 \pm 0.02\ s^{-1}$, and $K_d^K = 2.7 \pm 0.4$ μM. The value of K_d^K found indicates that BK_{Ca} channels bind K^+ fivefold tighter than previously thought (Neyton and Miller, 1988a).

Our value of k_{ext} was determined at 0 mV applied voltage. Neyton and Miller (1988a) found that in a solution containing "0" external K^+ (<5 μM) and 150 mM Na^+, k_{ext} increased e-fold with every 27-mV depolarization. At 50 mV, in the presence of external 150 mM NMDG and contaminating K^+, they measured a $k_{ext} = 20\ s^{-1}$. Using the expression $k_{ext}(V) = k_{ext}(0)\exp(V/27)$, we find that if $k_{ext}(0)$ is 7.6, then $k_{ext}(50)$ is 48 s^{-1}, which is 2.4× larger than the value found by Neyton and Miller (1988a). The larger value we predict is due to the reduction in the background contaminating [K^+] by the addition of the crown ether to the external solution.

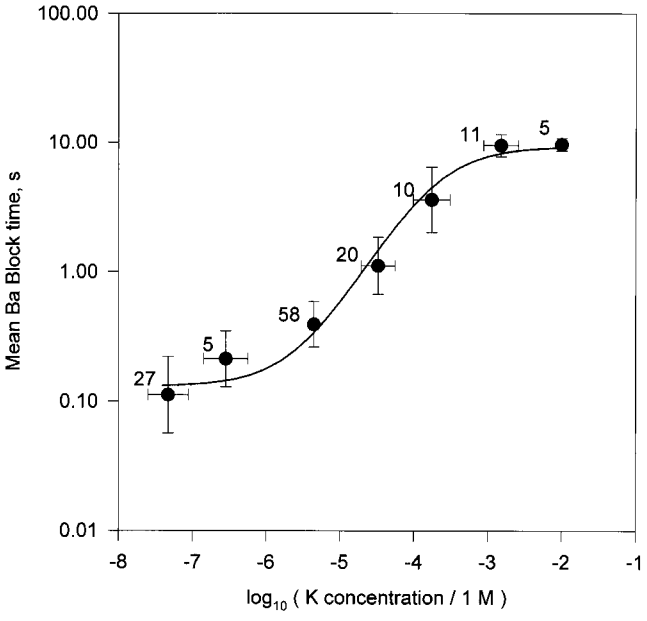

Figure 2. Mean slow Ba^{2+} block time as a function of $[K^+]_{ext}$. $[K^+]_{ext}$ was increased from the basal contaminating level (4.4 μM) by adding aliquots of 3 M KCl or decreased by adding 18C6TA to the external solution. Observations were grouped in decades of external K^+ concentration. The mean Ba^{2+} blocked time values are the average of 5–28 measurements in different single-channel membranes. The solid line is the best fit to the data using Eq. 1 with $k_{in} = 0.11 \pm 0.02\ s^{-1}$, $k_{ext} = 7.6 \pm 1.2\ s^{-1}$, and $K_d^K = 2.7 \pm 0.8$ μM.

K_d^K is also voltage dependent and Neyton and Miller (1988b) showed that the external lock-in site senses 18% of the voltage drop measured from the outside. Using the expression $K_d^K(V) = K_d^K(0)\exp(-z\delta eV/kT)$ with $z\delta = 0.18$ and a $K_d^K(0) = 2.7$ μM, we find that $K_d^K(50) = 3.9$, a value fivefold lower than the K_d^K of 19 μM determined by Neyton and Miller (1988a). Hence, by examining a wider range of external [K^+]s and using 18C6TA, we have been able to determine k_{ext} and K_d^K with more precision.

Fast component of the closed dwell-time distribution. The fast component of the closed dwell-time distribution was also modified by external [K^+]. As in the case of the slow Ba^{2+} block, the number of events increased as the external [K^+] concentration was reduced (see dwell time histograms in Fig. 1). However, in contrast to the slow component, the mean fast blocked time of the fast component of the closed time histogram is almost unchanged by a 10-fold reduction in the external [K^+]. Is the difference in slow and fast dwell-time dependence on [K^+] due to a modification of channel gating proper or is it the manifestation of a Ba^{2+} flickering block? (e.g., Sohma et al., 1996). To answer this question, we added crown ether to the internal side of the channel to a final concentration of 225 μM. This experimental maneuver decreases the internal [Ba^{2+}] from 70 to 5 nM, decreases the number of fast closed events by 30%, and increases P_o by 18% (from 0.6 to 0.73). The number of fast block events per unit open time, N_B, is predicted to be

$$N_B = k_{on}[Ba^{2+}]P_o, \qquad (2)$$

where k_{on} is the association rate constant for Ba^{2+} binding, and P_o the probability of opening. Therefore, a 14-fold decrease in [Ba^{2+}], considering the P_os before and after the addition of Ba^{2+}, should induce a 90% decrease in N_B. The theoretically expected decrease in N_B after lowering $[Ba^{2+}]_{int}$ is much more pronounced than the one found experimentally. This analysis suggests that upon diminishing $[K^+]_{ext}$, the increase in N_B is only partly due to a Ba^{2+} flickering block and that the reduction in external K^+ also induces the appearance of fast closed events.

The long-lasting closed state. Occupancy of the outer mouth of the pore of *Shaker* K^+ channels by K^+ slows the rate of C-type inactivation (López-Barneo et al., 1993). The site at which K^+ directly slows down inactivation appears to be a high-affinity binding site involved in the ionic selectivity mechanism (Kiss and Korn, 1998). In

fact, this site appears to be located in the neighborhood or in the channel selectivity filter, and Kiss et al. (1999) have argued that the selectivity filter itself is the inactivation gate. Since the selectivity filter is highly conserved among different K^+ channels, it is pertinent to ask why an inactivated state has not been previously observed in the BK_{Ca} channel even at very low $[K^+]$.

The single-channel current recorded at 0.09 μM K^+ in Fig. 1 shows a closed state of very long duration. Fig. 3 A shows that the channel enters this nonconducting state of very long duration when the $[K^+]_{ext}$ is reduced from the contaminating level (4.4 μM; Fig. 3 A, top) to 0.01 μM by the addition of crown ether to the external solution (Fig. 3 A, middle). After spending several minutes in the quiescent state, normal channel activity was recovered by adding K^+ to the external side to a final concentration of 10 μM (Fig. 3 A, bottom). The recovery of channel activity after a drastic reduction in external $[K^+]$ occurred in 15 of 22 trials. It appears then that the BK_{Ca} channel conductance collapses at external $[K^+]$s much lower than those necessary to arrest other K^+ channels.

Lithium, Na^+, Rb^+, Cs^+, and NH_4^+ were also tested for their abilities to recover the BK_{Ca} channel from its long-lasting nonconductive state. Rubidium (20 mM), Cs^+ (20 mM), and NH_4^+ (3.5–50 mM) were able to recover the channel from the nonconducting state. Fig. 3 B shows an example of recovery from the quiescent state when NH_4^+ is added to the external solution to a final concentration of 10 mM. Sodium (20–40 mM) and Li^+ (20–100 mM) were not able to recover channel activity, suggesting that only permeant cations are able to recover the channel from the conformation it adopts at very low $[K^+]$.

External TEA^+ Traps K^+ Inside BK_{Ca} Channels

In *Shaker* K^+ channels, one specific amino acid location in the pore-forming region (position 449) is crucial in determining sensitivity to external TEA^+ (MacKinnon and Yellen, 1990; Kavanaugh et al., 1991). An aromatic residue at the 449 position is a requirement for high affinity TEA^+ blockade and Heginbotham and MacKinnon (1992) showed that a bracelet of pore-lining tyrosines forms the high affinity TEA^+ receptor. BK_{Ca} channels are also blocked by TEA^+ and they show a high affinity for this quaternary ammonium ion (Blatz and Magleby, 1984; Vergara et al., 1984; Yellen, 1984a). In BK_{Ca} channels, there is a tyrosine residue at a position corresponding to the TEA^+-sensitive position in *Shaker* K^+ channels (Adelman et al., 1992). We reasoned that since a TEA^+ binding site in BK_{Ca} channels is structurally well defined (Shen et al., 1994), it would be of interest to see whether or not TEA^+ behaves as a lock-in ion like external K^+.

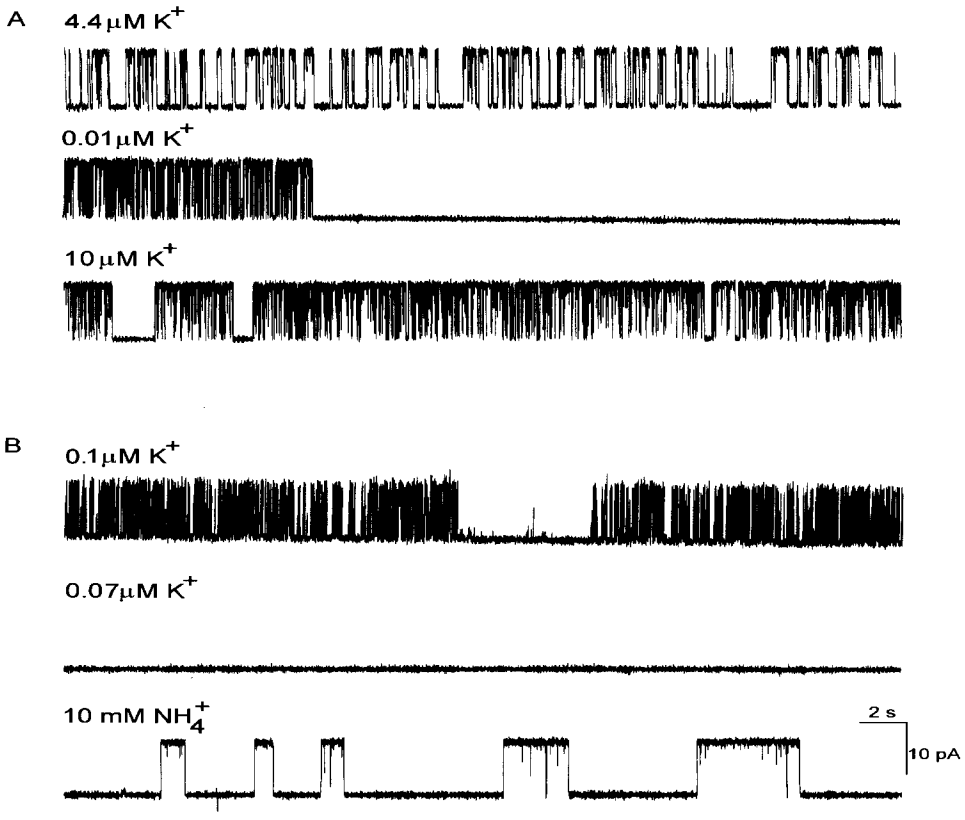

Figure 3. The very long lasting nonconducting state is reversibly modulated by permeant ions. (A) The three current traces were obtained at 0 mV with 4.4, 0.01, and 10 μM external K^+, respectively. When $[K^+]_{ext}$ was reduced to 0.01 μM by the addition of 2.4 mM crown ether, the channel entered into a nonconducting state that lasted several minutes. Upon increasing free $[K^+]_{ext}$ to 10 μM by the addition of 1.5 mM KCl, normal channel activity was recovered. (B) The first trace was obtained at 0 mV with 0.1 μM external K^+ attained by the addition of 2.4 mM crown ether; at this $[K^+]_{ext}$, the long lasting closed state separates bursts of channel activity. No openings occurred for a 10-min time period after reducing $[K^+]_{ext}$ to 0.07 μM by the addition of crown ether to a final concentration of 3.5 mM. Channel activity recovered after adding ultra pure 10 mM NH_4Cl to the external solution. Internal $[Ba^{+2}]$ was estimated to be 70 nM in both experiments.

Since we expected TEA^+ to increase Ba^{2+} mean blocked time, we reduced $[K^+]_{ext}$ to begin the experiment with short mean Ba^{2+} block time. The crown ether concentration was adjusted to decrease the potassium concentration from the basal level down to values where the channels would not enter into the long lasting nonconducting state. Furthermore, TEA^+ seems to protect the channel from falling into the long lasting closed state since we observed stable channel activity with $[K^+]_{ext}$ as low as 0.007 μM. In the experiment shown in Fig. 4, we reduced the external $[K^+]$ concentration from 6 to 0.03 μM by adding 0.9 mM crown ether to the external solution. The figure shows the effect of external TEA^+ on the nonconducting dwell times induced by the presence of internal Ba^{2+}. TEA^+ reduces the open channel current and also increases the duration of the closed dwell times. In the absence of TEA^+, the measured mean block time was 160 ms; after increasing the external TEA^+ to 900 μM, the mean block time increased to 1,700 ms.

Surprisingly, if external $[K^+]$ is reduced from 0.06 to 0.007 μM by the addition of crown ether, in the presence of external TEA^+, the mean block time is decreased (Fig. 5). Fig. 5, middle and bottom, shows that channel conductance is not affected by the addition of crown ether. Therefore, the complexing agent does not affect TEA^+ concentration.

Fig. 6 shows that the effect of TEA^+ on Ba^{2+} block strongly depends on external K^+ concentration. In the presence of 130 μM external K^+, 2 mM TEA^+ brings the mean Ba^{2+} blocked time to ~20 s. Therefore, the blocked time is even longer than the maximum value expected for Ba^{2+} leaving toward the internal side of the channel in the presence of high external $[K^+]$(compare Fig. 2). However, in the presence of 0.04 μM K^+, the same TEA^+ concentration induces a mean Ba^{2+} blocked time of only 2 s.

A Possible Model

The ability of external TEA^+ to slow down Ba^{2+} dissociation cannot be reconciled with the idea that TEA^+ and K^+ compete for the same binding site in the channel or with the simple picture of ion–ion repulsion within the pore. In both cases, it is expected that TEA^+ should behave less effective as a lock-in ion in the presence of K^+.

To interpret our results quantitatively, we propose the model illustrated in Fig. 7. The channel is viewed as having three sites: a Ba^{2+}-blocking site, a K^+-binding site located externally to the blocking site, and the external TEA^+ site. As shown by Neyton and Miller (1988a) and documented in Fig. 2, at very low $[K^+]$ and in the absence of external TEA, Ba^{2+} can dissociate and exit to the external solution with a rate (k_{ext}) much greater than the exit rate toward the internal side (k_{in}) (Fig. 7). The results shown in Fig. 2 were interpreted in terms of an increase in the occupancy of an external K^+ site as the external $[K^+]$ was increased (S2 in Fig. 7). The model proposes that TEA^+ can bind to the singly or doubly occupied channel. Therefore, TEA^+ can trap K^+ inside the pore and the blocking Ba^{2+} ion must then either dissociate to the internal solution, or wait for the TEA^+ and K^+ sites to become empty. Assuming that the unblock–block reactions are slow compared with the K^+ and TEA^+ binding reactions, the model presented in Fig. 7 predicts the following relation for the mean Ba^{2+} blocked time, $\tau_{o\text{-}B\alpha}$:

$$\tau_{0-B\alpha} = [k_{in}P_{Ba-K-S3} + k_{in(K,TEA)}P_{Ba-K-TEA} + k_{in(TEA)}P_{Ba-S2-TEA} + (k_{ext} + k_{in})P_{Ba-S2-S3}]^{-1}, \quad (3)$$

where P_{Ba}, $P_{Ba\text{-}K}$, $P_{Ba\text{-}TEA}$, and $P_{Ba\text{-}K\text{-}TEA}$ are the probabilities of finding the channel occupied by Ba^{2+} only, by Ba^{2+} and K^+, by Ba^{2+} and TEA^+, or by Ba^{2+}, K^+, and

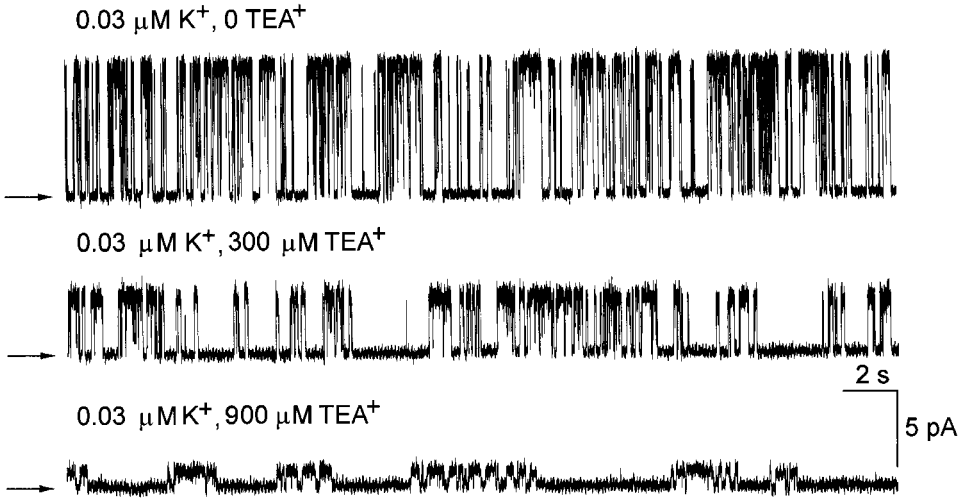

Figure 4. External TEA^+ causes an increase in the Ba^{2+} block time. All three traces were recorded with 0.03 μM external $[K^+]$ and 170 nM internal Ba^{2+}. In the absence of TEA^+, the mean Ba^{2+} blocked time was 160 ms (top); with 300 μM TEA^+, mean block time was 430 ms (middle); and with 900 μM TEA^+, mean block time was 1,700 ms (bottom).

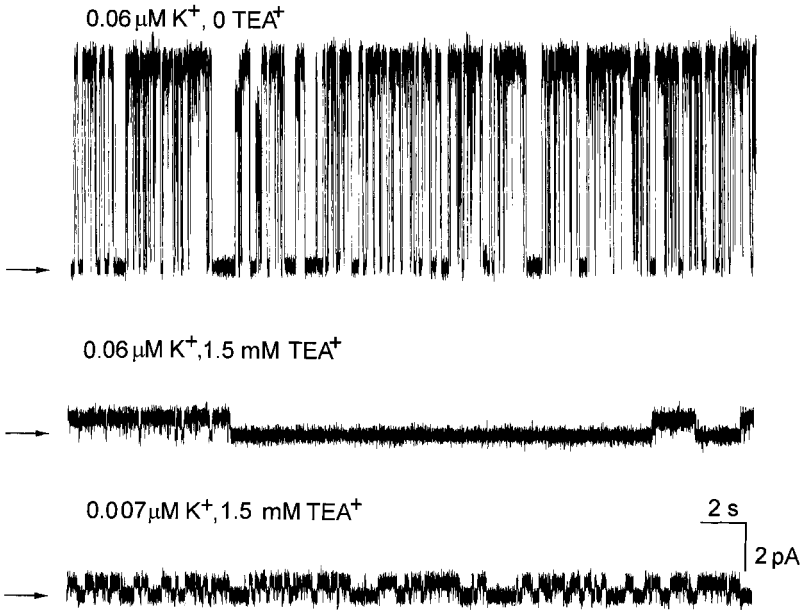

Figure 5. External TEA^+ effect on mean Ba^{2+} block time depends on $[K^+]_{ext}$. The top single-channel current record was obtained in the absence of TEA^+ and in 0.06 μM K^+_{ext}. In this experiment, the K^+ contamination level was 4 μM, and 0.06 μM K^+_{ext} was reached by adding crown ether to a final concentration of 500 μM. The mean Ba^{2+} blocked time was 200 ms. (Middle) With 1.5 mM external TEA^+ and 0.06 μM K^+_{ext}, mean Ba^{2+} blocked time increased to 3,220 ms. The internal $[Ba^{2+}]$ was 70 nM. (Bottom) The internal $[Ba^{2+}]$ was 220 nM and $[K^+]_{ext}$ was reduced to 7 nM by adding 18C6TA to a final concentration of 4 mM. Under these experimental conditions, mean blocked time was 190 ms.

TEA^+, respectively. These probabilities are given by the following relationships:

$$P_{Ba-S2-S3} = \{1 + ([K^+]/K_d^{K})(1 + [TEA]/K_{d1}^{TEA}) + [TEA]/K_{d2}^{TEA}\}^{-1} \quad (4a)$$

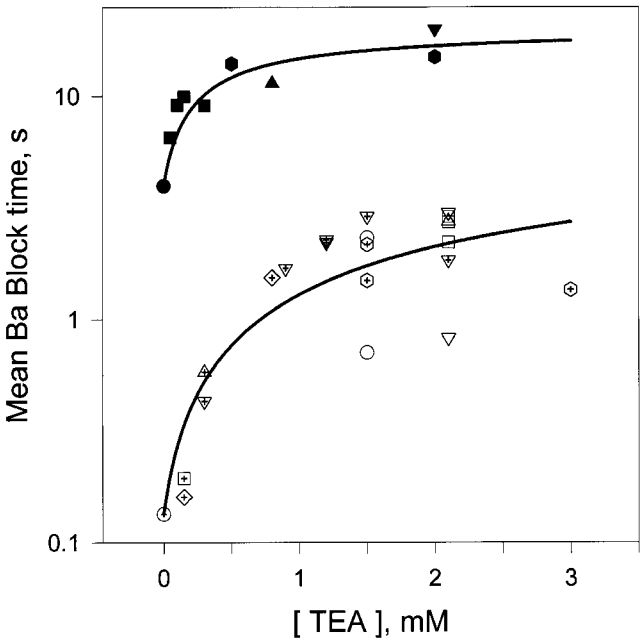

Figure 6. Mean Ba^{2+} block time as a function of $[TEA^+]$ at two external K^+ concentrations. Mean Ba^{2+} block times measured with 130 μM K^+ in four different single-channel membranes (closed symbols) and with 0.04 μM K^+ in nine different single-channel membranes (open symbols). The lines are fits to Eqs. 3 and 4 using $k_{ext} = 7.6\ s^{-1}$, $k_{in} = k_{in(K)} = 0.11\ s^{-1}$, $k_{in(TEA)} = 0.14\ s^{-1}$, $k_{in(K,TEA)} = 0.047\ s^{-1}$, $K_{d1}^{TEA} = K_{d2}^{TEA} = 94$ μM. The values of k_{ext}, $k_{in(K)}$, and K_d^K are the same as those used in Fig. 2. Free parameters were found using nonlinear curve fitting.

$$P_{Ba-K-S3} = [K^+]/\{[K^+] + K_d^{K}(1 + [TEA]/K_{d2}^{TEA}) + [K^+][TEA]/K_{d2}^{TEA}\} \quad (4b)$$

$$P_{Ba-S2-TEA} = [TEA]/\{[TEA] + K_{d2}^{TEA}(1 + [K^+]/K_d^{K})(1 + [TEA]/K_{d1}^{TEA})\} \quad (4c)$$

$$P_{Ba-K-TEA} = [TEA]/\{[TEA] + K_{d1}^{TEA}(1 + [K^+]/K_d^{K})(1 + [TEA]/K_{d2}^{TEA})\}, \quad (4d)$$

where K_d^K is the dissociation constant for K^+, K_{d1}^{TEA} is the dissociation constant for TEA^+ from the triply occupied state, and K_{d2}^{TEA} is the dissociation constant for TEA^+ from the doubly occupied state. There are five different rate constants for Ba^{2+} exit: k_{ext} is the rate of exit to the extracellular side when the channel is occupied only by a Ba^{2+} ion, k_{in} is the rate constant of exit to the intracellular side when the channel is occupied only by a Ba^{2+} ion, and $k_{in(K)}$, $k_{in(TEA)}$, $k_{in(K,\ TEA)}$ are the rate constants of exit toward the extracellular side when the channel is occupied by Ba^{2+} and K^+, by Ba^{2+} and TEA^+, or by Ba^{2+}, K^+, and TEA^+, respectively.

The model accommodates rate constants for Ba^{2+} exit toward the internal side that are different (compare Figs. 2 and 6) in the absence and presence of TEA^+. Experimentally, we found that when the quaternary ammonium ion and K^+ are present in the external solution, $k_{in(K,TEA)}$ is approximately twofold slower than in the absence of TEA. On the other hand, the fit to the data with the model shown in Fig. 7 indicates that in the absence of K^+, the rate constant for Ba^{2+} exit, $k_{in(TEA)}$, is approximately four times larger than $k_{in(K,TEA)}$ (see Fig. 6). We have tested our model by comparing the measured mean Ba^{2+} blocked times at

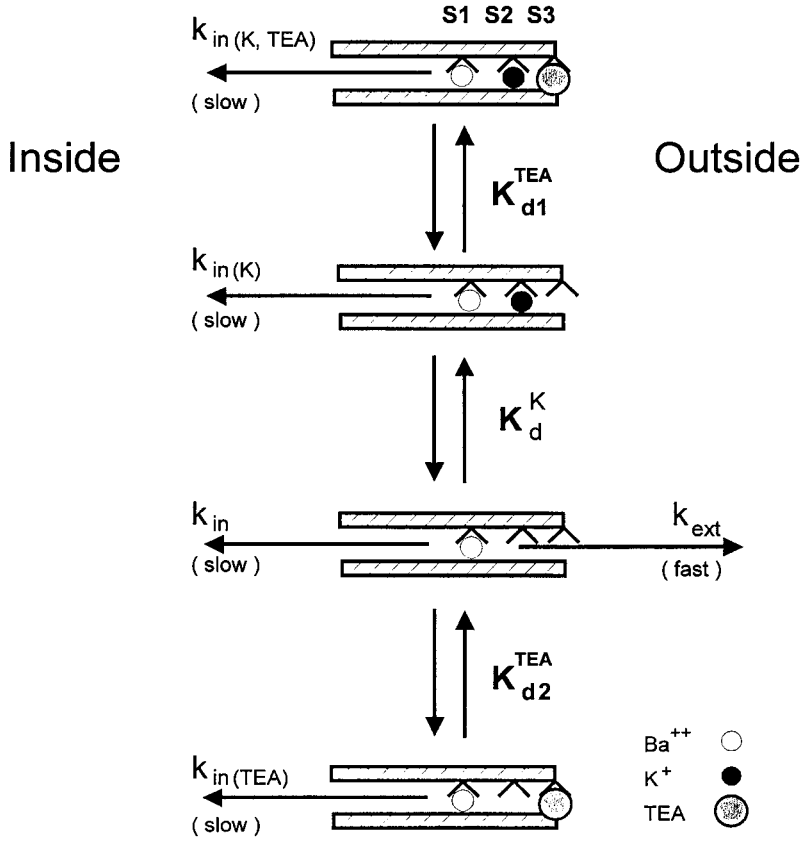

Figure 7. Pictorial representation of the possible routes of exit of Ba^{2+} from the channel. There are three ion-binding sites in the channel named S1, S2, and S3. S1 is the Ba^{2+} site, S2 is the lock-in site of Neyton and Miller (1988a), and S3 is the TEA^+ site. K_d^K is the dissociation constant for K^+, K_{d1}^{TEA} is the dissociation constant for TEA^+ from the triple-occupied channel, and K_{d2}^{TEA} is the dissociation constant for TEA^+ from the double-occupied state. There are five different rate constants for Ba^{2+} exit from the channel: k_{ext} is the rate of exit to the extracellular side, k_{in} is the rate constant for the exit toward the intracellular side when the channel is occupied by Ba^{2+} only, $k_{in(K)}$, $k_{in(TEA)}$, and $k_{in(K, TEA)}$ are the rate constants for exit toward the intracellular side from the channel occupied by Ba^{2+} and K^+, Ba^{2+} and TEA^+, and Ba^{2+}, K^+, and TEA^+, respectively.

different $[K^+]$ and $[TEA^+]$ from 26 different single-channel membranes with the calculated mean blocked times obtained using Eq. 3. The model proposed in Fig. 7 describes the data rather well (Fig. 8 A). The model is unable to predict the experimental results if triple occupancy is not allowed ($K_{d1}^{TEA} = \infty$) (Fig. 8 B) or if TEA^+ is unable to bind the channel unless it is occupied by K^+ ($K_{d2}^{TEA} = \infty$) (Fig. 8 C). Fig. 8 B shows that if triple occupancy is not allowed, the model predicts an attenuated effect of TEA^+ on the mean Ba^{2+} blocked time relative to that found experimentally. On the other hand, Fig. 8 C illustrates that if TEA^+ can only bind to the Ba^{2+}-occupied channel in a triple occupancy configuration (when the lock-in site for K^+ is full), then the model fails to account for the data obtained at very low $[K^+]$. The best correlation between model generated and experimental values of the mean Ba^{2+} block time was obtained when TEA^+ binding was allowed in any configuration of the model with rate constants of $K_{d1}^{TEA} = 180$ μM and $K_{d2}^{TEA} = 67$ μM. It is very interesting that the ratio between these two dissociation constants (2.5) reveals a K^+–TEA^+ repulsion of ~0.6 kcal/mol. This very low repulsion energy implies that the bound TEA^+ ion is essentially shielded from the K^+ ion occupying the external lock-in site.

The kinetics of block by TEA^+ are rapid, operating in the time scale of microseconds (Blatz and Magleby, 1984; Vergara et al., 1984; Yellen, 1984a; Villarroel et al. 1988); therefore, the TEA^+ blocking events are too fast to be directly observed since they are filtered by the measuring electronics. Therefore, TEA^+ appears to reduce the observed channel current (Figs. 4 and 5). Because of this effect, the ratio between the average single-channel current value in the absence of TEA^+, i_o, and its value in the presence of the quaternary ammonium ion, $\langle i \rangle$, is a measure of the channel occupancy by TEA^+ at its blocking site:

$$i_0/\langle i \rangle = (1 + [TEA^+]/K_d^{TEA}). \quad (5)$$

Since in this case TEA^+ blocks a channel containing only K^+ ions in its conduction machinery, it is pertinent to ask whether the dissociation constant for TEA^+, K_d^{TEA}, is similar to that obtained from its effect on the mean Ba^{2+} block time.

Fig. 9 illustrates the dependence of the channel current on TEA^+ concentration at 0 mV and in different $[K^+]$ (each symbol represents a different $[K^+]$). There is a linear relationship that is well described by Eq. 5 with a $K_d^{TEA} = 106$ μM (Fig. 9, solid line). Notice that the fit to Eq. 5 is reasonably good for all the $[K^+]$ tested, indicating that there is not a single hint of competition between K^+ and TEA^+ for a site(s). Moreover, the value of $K_d^{TEA^+}$ obtained is very similar to that ob-

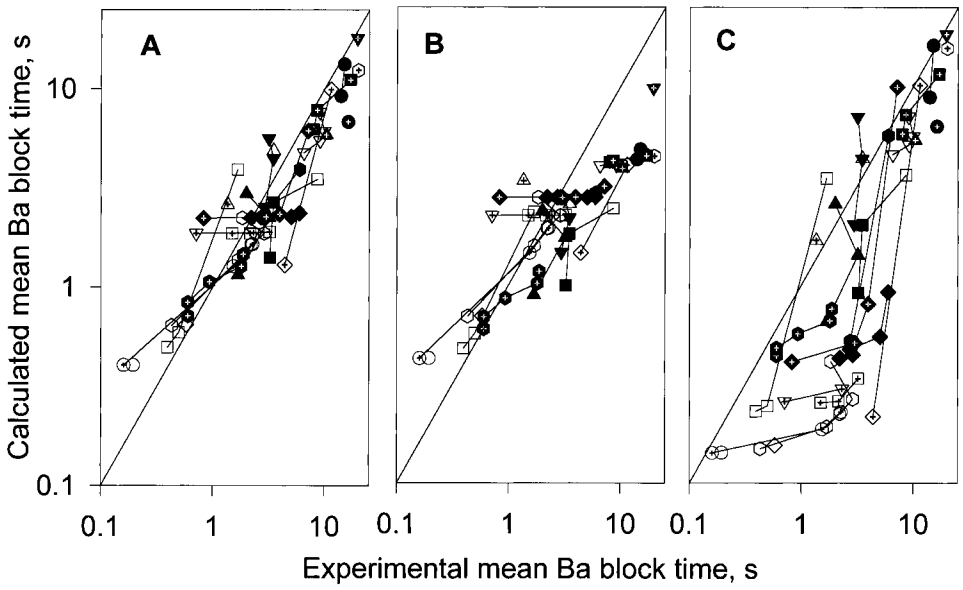

Figure 8. Comparison of experimental results with predictions of the model: the effects of K^+ and TEA^+ on mean Ba^{2+} block times. The vertical axis represents the mean Ba^{2+} blocked time calculated with the model for various [K^+] and [TEA^+], the horizontal axis represents the experimental mean Ba^{2+} block time measured at the same [K^+] and [TEA^+]. Each symbol represents a different single-channel membrane and data points belonging to the same membrane were connected with straight lines. (A) Calculated values were obtained by solving Eqs. 3 and 4 using the following parameters: k_{ext} = 7.6 s^{-1}, k_{in} = $k_{in(K)}$ = 0.11 s^{-1}, $k_{in(TEA)}$ = 0.22 s^{-1}, $k_{in(K,TEA)}$ = 0.051 s^{-1}, K_{d1}^{TEA} = 180, and K_{d2}^{TEA} = 67 μM. The values of k_{ext}, $k_{in(K)}$, and K_d^K are those determined in Fig. 2. The other parameters were chosen to give the best correlation between theory and experiment; i.e., the minimum deviation from the identity line. (B) The model was restricted by not allowing the triple-occupied state. This restriction fails to account for the longest mean block times measured at high [K^+]. (C) The model was restricted by allowing TEA^+ binding to the channel only when K^+ is present in the lock-in site. This TEA restriction fails to account for the shortest block times obtained at low [K^+].

tained by Villarroel et al. (1988) (120 μM) under symmetrical 100-mM KCl conditions.

discussion

The crystal structure of the K^+ channel pore from *Streptomyces lividans* revealed two binding sites for potassium in the selectivity filter that are ~0.75-nm apart (Doyle et al., 1998). In this channel, like in the BK_{Ca} channel, the TEA^+ binding site is comprised of four tyrosines located externally to the outer K^+ binding site (Heginbotham and MacKinnon, 1992). Since TEA^+ can trap K^+ ions inside BK_{Ca} channels, we assigned lock-in site to the outer K^+ binding site described by Doyle et al. (1998). Since the crystal radius of Ba^{2+} is similar to the crystal radius of K^+, Ba^{2+} probably occupies the inner site. A third site was identified at the pore center in a large cavity (Doyle et al., 1998). An ion is stabilized in this central position by the aqueous environment and by α helical structures pointing their partial negative charge toward the cavity where the ion is located. We hypothesize that the Ba^{2+} flickering block originates from Ba^{2+} entering and leaving the pore from the pore cavity.

In the case of potassium channels, it is clear that permeating ions within the conduction pathway affect some of the structural changes associated with gating

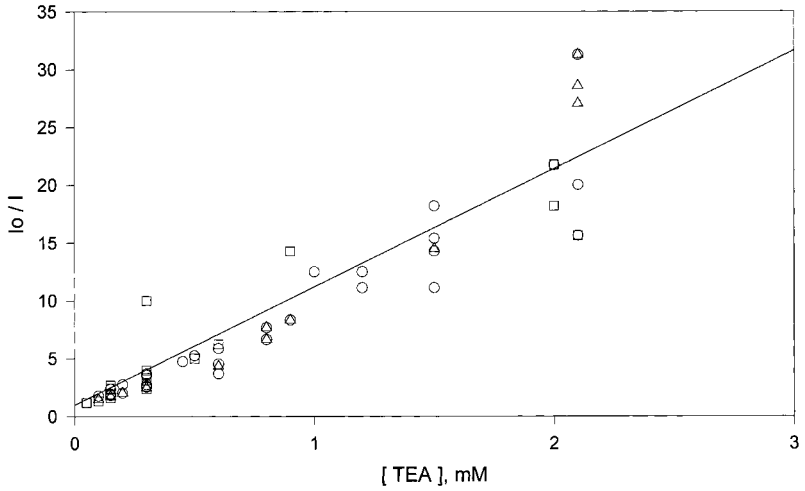

Figure 9. Dissociation constant of TEA^+ measured from the amplitude of the single channel current. This plot contains data from 30 single channel membranes. Symbols represent different external K^+ concentrations: (○) 0.04–1, (△) 4–10, and (□) 100–130 μM. The solid line is the best fit of the data with Eq. 5 using a dissociation constant of 95 ± 5 μM.

(Almers and Armstrong, 1980; Pardo et al., 1992; Gómez-Lagunas, 1997; Jåger et al., 1998; Melishchuck et al., 1998) and C-type inactivation (López-Barneo et al., 1993; Levy and Deutsch, 1996; Kiss and Korn, 1998). Squid axon K^+ channels become nonfunctional when K^+ is removed from the internal and external solutions, but these channels can survive in an internal K^+-free solution if external K^+, Cs^+, NH_4^+, or Rb^+ ions are present (Almers and Armstrong, 1980). *Shaker* K^+ channels in K^+-free solutions become irreversibly nonconducting, but only after opening. This long-lasting state can be entered only if there is inward gating charge movement (Melishchuck et al., 1998). *Shaker* K^+ channels can be protected against the deleterious effects of the absence of K^+ by mutations that remove C-type inactivation. On the other hand, some mammalian delayed rectifier K^+ channels remain stable after removal of internal and external K^+ and become permeable to Na^+ ions (e.g., Kiss et al., 1998).

The data presented here shows that occupancy of a very high affinity site for K^+, most likely the lock-in site, controls ion permeation in the BK_{Ca} channel. Emptying the channel of K^+ ions could lead to the equivalent of the C-type inactivation or to the K^+ conductance collapse phenomena described for other K^+ channels. When the lock-in site is empty, the channel clearly undergoes structural changes that lead finally to the long-lasting inactivated state. These changes are probably triggered by electrostatic repulsion of the carbonyl groups, which makes the selectivity filter atoms move apart. Fig. 2 shows that the K_d^K for the lock-in site is 2.7 μM, which corresponds to an energy well of −13 kT. Considering that this value of K_d^K is for the double occupied [K^+–Ba^{2+}] channel, this energy is an upper limit that indicates that the binding of K^+ to BK_{Ca} channels as tight as the binding of Ca^{2+} to Ca^{2+} channels (e.g., Dang and McCleskey, 1998). On the other hand, the ratio of the rate constants k_{ext}/k_{in} is 100 and this implies that Ba^{2+} must jump an energy barrier 2.8 kcal/mol larger when leaving the channel toward the internal side.

Although we do not know the details of the molecular mechanism that governs C-type inactivation, it is known that external TEA^+, K^+, and other monovalent cations inhibit it. Point mutations in *Shaker* K^+ channels have also shown that the rate of C-type inactivation and the K^+ permeability properties can be altered simultaneously (López-Barneo et al., 1993). The general explanation of this phenomenon is that occupancy of a site by K^+ or other permeant cations hinders the C-type inactivation conformational change, probably a collapse of the selectivity filter (Kiss and Korn, 1998). We have demonstrated here that TEA^+ binds to the Ba^{2+}-blocked channel when the lock-in site is occupied by K^+, and prevents K^+ from leaving this site. This turns TEA^+ into an ion that can protect the channel from C-type inactivation, by binding to a site different from the typical lock-in site. Considering that K^+ protects BK_{Ca} channels from entering into a very stable nonconducting state, how is it that the BK_{Ca} channel is not protected by the internal K^+ ions flowing through it? Our results suggest that Ba^{2+} cuts off potassium flow to the external K^+ site. During a Ba^{2+} block at very low $[K^+]_{ext}$, the channel has two possibilities when the lock-in site is empty: (a) it can enter a long lasting nonconducting state leaving the Ba^{2+} trapped inside or (b) Ba^{2+} can occupy the lock-in site and exit the channel toward the external side, making the channel enter into a burst of activity. A similar effect of extracellular K^+ and internal blockade has been shown in *Shaker* K^+ channels (Baukrowitz and Yellen, 1996). In this case, a hydrophobic TEA^+ analogue applied internally hindered the potassium flow to a site in the pore and thereby greatly increased the rate of C-type inactivation. Internal TEA^+ also prevents the refilling of the pore by K^+ in the case of the potassium channel of the squid axon (Khodakhah et al., 1997). In the absence of external K^+, this produces an irreversible decrease of the K^+ current.

The effect of external K^+ on the ability of TEA^+ to lock Ba^{2+} into the channel was explained using a model in which Ba^{2+}, K^+, and TEA^+ can simultaneously occupy the channel. The analysis of our results demonstrated that TEA^+ binding to the Ba^{2+}-blocked channel is essentially the same whether or not a K^+ ion is bound and that the binding constant is not very different from the one obtained measuring the current amplitude in the presence of different [TEA^+] and [K^+]. This result implies that there is little electrostatic repulsion between the K^+ in the external lock-in site and the TEA^+ bound to its external receptor. The crystal structure of the K^+ channel from *Streptomyces lividans* showed that the distance separating the K^+ ion located in the external site of the selectivity filter and the TEA^+ ion is 0.8 nm (Doyle et al., 1998). Given this distance, the expected electrostatic repulsion is 41 kcal/mol if a nonpolarizable medium separates the two ions, or 2 kcal/mol if a medium with a dielectric constant of 20 separated the ions. The fact that the expected repulsion between these two ions is not detected by our experiments can only be explained if the K^+ ion in the lock-in site is shielded from the TEA^+. It is possible that the ring of aspartates located in position 295 in m*Slo* (Shen et al., 1994) supplies this shielding.

We thank Joan Haab and Dorine Starace for helpful comments on the manuscript.

This work was supported by Chilean grants FONDECYT 197-0739 (R. Latorre), 198-1053 (C. Vergara), and Cátedra Presi-

dencial and a group of Chilean companies (AFP PROTECTION, CODELCO, Empresas CMPC, CGE, Gener S.A., Minera Escondida, Minera Collahuasi, NOVAGAS, Business Design Association, and XEROX Chile) and a grant from Human Frontiers in Science Program (to R. Latorre).

Submitted: 20 January 1999 Revised: 26 June 1999 Accepted: 29 June 1999

references

Adelman, J.P., K.Z. Shen, M.P. Kavanaugh, R.A. Warren, Y.N. Wu, A. Lagrutta, C.T. Bond, and R.A. North. 1992. Calcium-activated potassium channels expressed from cloned complementary DNAs. *Neuron*. 9:209–216.

Almers, W., and C.M. Armstrong. 1980. Survival of K^+ permeability and gating currents in squid axons perfused with K^+-free media. *J. Gen. Physiol.* 75:61–78.

Alvarez, O., A. Villarroel, and G. Eisenman. 1992. Calculation of ion currents from energy profiles and energy profiles from ion currents in a multibarrier, multisite, multioccupancy channel model. *Methods Enzymol.* 207:816–854.

Baukrowitz, T., and G. Yellen. 1996. Use-dependent blockers and exit rate of the last ion from the multi-ion pore of a K^+ channel. *Science.* 271:653–656.

Blatz, A.L., and K.L. Magleby. 1984. Ion conductance and selectivity of single calcium-activated potassium channels in cultured rat muscle. *J. Gen. Physiol.* 84:1–23.

Candia, S., M.L. Garcia, and R. Latorre. 1992. Mode of action of iberiotoxin, a potent inhibitor of the large conductance Ca^{2+}-activated K^+ channel. *Biophys. J.* 63:583–590.

Cecchi, X., D. Wolff, O. Alvarez, and R. Latorre. 1987. Mechanisms of Cs^+ blockade in a Ca^{2+}-activated K^+ channel from smooth muscle. *Biophys. J.* 52:707–716.

Dang, T.X., and E.W. McCleskey. 1998. Ion channel selectivity through stepwise changes in binding affinity. *J. Gen. Physiol.* 111: 185–193.

Díaz, F., M. Wallner, E. Stefani, L. Toro, and R. Latorre. 1996. Interaction of internal Ba^{2+} with a cloned Ca^{2+}-dependent K^+ (h*slo*) channel from smooth muscle. *J. Gen. Physiol.* 107:399–407.

Dietrich, B. 1985. Coordination chemistry of alkali and alkali-earth cations with macrocyclic ligands. *J. Chem. Ed.* 62:954–964.

Doyle, D.A., J.M. Cabral, R.A. Pfuetzner, A. Kuo, J.M. Gulbis, S.L. Cohen, B.T. Chait, and R. MacKinnon. 1998. The structure of the potassium channel: molecular basis of K^+ conduction and selectivity. *Science.* 280:69–77.

Eisenmann, G., R. Latorre, and C. Miller. 1986. Multi-ion conduction and selectivity in the high-conductance Ca^{++}-activated K^+ channel from skeletal muscle. *Biophys. J.* 50:1025–1034.

Gómez-Lagunas, F. 1997. *Shaker* B K^+ conductance in Na^+ solutions lacking K^+ ions: a remarkably stable non-conducting state produced by membrane depolarizations. *J. Physiol.* 449:3–15.

Heginbotham, L., and R. MacKinnon. 1992. The aromatic binding site for tetraethylammonium ion on potassium channels. *Neuron*. 8:483–491.

Hodgkin, A.L., and R.D. Keynes. 1955. The potassium permeability of a giant nerve fiber. *J. Physiol.* 128:61–88.

Jåger, H., H. Rauer, A.N. Nguyen, J. Aiyar, K.G. Chandy, and S. Grissner. 1998. Regulation of mammalian *Shaker*-related K^+ channels: evidence for non-conducting closed and non-conducting inactivated states. *J. Physiol.* 506:291–301.

Kavanaugh, M.P., M.D. Varnum, P.B. Osborne, M.J. Christie, A.E. Busch, J.P. Adelman, and R.A. North. 1991. Interaction between tetraethylammonium and amino acid residues in the pore of cloned voltage-dependent potassium channels. *J. Biol. Chem.* 266: 7583–7587.

Kiss, L., D. Immke, J. Loturco, and S.J. Korn. 1998. The interaction of Na^+ and K^+ in voltage-gated potassium channels: evidence for cation binding sites of different affinity. *J. Gen. Physiol.* 111:195–206.

Kiss, L., and S.J. Korn. 1998. Modulation of C-type inactivation by K^+ at the potassium channel selectivity filter. *Biophys. J.* 74:1840–1849.

Kiss, L., J. Lo Turco, and S.J. Korn. 1999. Contribution of the selectivity filter to inactivation in potassium channels. *Biophys. J.* 76: 253–263.

Khodakhah, K., A. Melishchuck, and C.M. Armstrong. 1997. Killing K^+ channels with TEA^+. *Proc. Natl. Acad. Sci. USA.* 94:13335–13338.

Latorre, R., C. Vergara, and C. Hidalgo. 1982. Reconstitution in planar lipid bilayers of a Ca^{2+}-dependent K^+ channel from transverse tubule membranes isolated from rabbit skeletal muscle. *Proc. Natl. Acad. Sci. USA.* 79:805–809.

Levy, D.I., and C. Deutsch. 1996. Recovery from C-type inactivation is modulated by extracellular potassium. *Biophys. J.* 70:798–805.

López-Barneo, J., T. Hoshi, S.F. Heinemann, and R.W. Aldrich. 1993. Effects of external cations and mutations in the pore region on C-type inactivation of *Shaker* potassium channels. *Receptors Channels.* 1:61–71.

Melishchuck, A., A. Loboda, and C.M. Armstrong. 1998. Loss of *Shaker* K channel conductance in 0 K^+ solutions: role of the voltage sensor. *Biophys. J.* 75:1828–1835.

MacKinnon, R., and G. Yellen. 1990. Mutations affecting TEA blockade and ion permeation in voltage-activated K^+ channels. *Science.* 250:276–279.

Miller, C., R. Latorre, and I. Reisin. 1987. Coupling of voltage-dependent gating and Ba^{2+} block in the high conductance Ca^{2+}-activated K^+ channel. *J. Gen. Physiol.* 90:427–449.

Moczydlowski, E., and R. Latorre. 1983. Gating kinetics of Ca^{2+}-activated K^+ channels from rat muscle incorporated into planar lipid bilayers. Evidence for two voltage-dependent Ca^{2+} binding reactions. *J. Gen. Physiol.* 82:511–542.

Neyton, J. 1996. A Ba^{2+} chelator suppresses long shut events in fully activated high-conductance Ca^{2+}-dependent K^+ channels. *Biophys. J.* 71:220–226.

Neyton, J., and C. Miller. 1988a. Potassium blocks barium permeation through a calcium-activated potassium channel. *J. Gen. Physiol.* 92:549–568.

Neyton, J., and C. Miller. 1988b. Discrete Ba^{2+} blockade as a probe of ion occupancy and pore structure in the high-conductance Ca^{2+} activated K^+ channel. *J. Gen. Physiol.* 92:569–586.

Pardo, L.A., S.H. Heinemann, H. Trelau, U. Ludewig, C. Lorra, O. Pongs, and W. Stühmer. 1992. Extracellular K^+ specifically modulates a rat brain K^+ channel. *Proc. Natl. Acad. Sci. USA.* 89:2466–2470.

Shen, K.-Z., A. Lagrutta, N.W. Davies, N.B. Standen, J.P. Adelman, and R.A. North. 1994. Tetraethylammonium block of *Slowpoke* calcium-activated potassium channels expressed in *Xenopus* oocytes: evidence for tetrameric channel formation. *Pflügers Arch.* 426:440–445.

Sohma, Y., A. Harris, C.J.C. Wardle, B.E. Argent, and M.A. Gray.

1996. Two barium binding sites on a maxi-K^+ channel from human vas deferens epitheliala cells. *Biophys. J.* 70:1316–1325.

Stampe, P., and T. Begenisich. 1996. Unidirectional K^+ fluxes through recombinant *Shaker* potassium channels expressed in single *Xenopus* oocytes. *J. Gen. Physiol.* 107:449–457.

Vergara, C., and R. Latorre. 1983. Kinetics of Ca^{2+}-activated K^+ channels from rabbit muscle incorporated into planar bilayers. Evidence for a Ca^{2+} and Ba^{2+} blockade. *J. Gen. Physiol.* 82:543–568.

Vergara, C., E. Moczydlowski, and R. Latorre. 1984. Conduction, blockade and gating in a Ca^{2+}-activated K^+ channel incorporated into planar lipid bilayers. *Biophys. J.* 45:73–76.

Villarroel, A., O. Alvarez, A. Oberhauser, and R. Latorre. 1988. Probing a Ca^{2+}-activated K^+ channel with quaternary ammonium ions. *Pflügers Arch.* 413:118–126.

Yellen, G. 1984a. Ionic permeation and blockade in Ca-activated K channels of bovine chromaffin cells. *J. Gen. Physiol.* 84:157–186.

Yellen, G. 1984b. Relief of Na^+ block of Ca^{++}-activated K^+ channels by external cations. *J. Gen. Physiol.* 84:187–199.